

# Nonlinear refraction dynamics of solvents and gases

Peng Zhao<sup>1</sup>, Matthew Reichert<sup>1,2</sup>, Trenton R. Ensley<sup>1,4</sup>, William M. Shensky III<sup>4</sup>, Andrew G. Mott<sup>4</sup>,  
David J. Hagan<sup>1,3</sup>, and Eric W. Van Stryland<sup>1,3</sup>

<sup>1</sup>CREOL, The College of Optics and Photonics, University of Central Florida, Orlando, FL, 32816, USA

<sup>2</sup>Current address: Department of Electrical Engineering, Princeton University, Princeton, New Jersey 08455

<sup>3</sup>Department of Physics, University of Central Florida, Orlando, FL, 32816, USA

<sup>4</sup>U.S. Army Research Laboratory, 2800 Powder Mill Rd., Adelphi, MD 20783-1138

## ABSTRACT

We present measurements of the temporal and polarization dependence of the nonlinear optical (NLO) response of selected organic solvents using our beam deflection (BD) method. These measurements allow us to separately determine the bound-electronic and nuclear responses which then determines the NLO response function. With this NLO response function the outcome of other experiments such as Z-scan as a function of pulsewidth can be predicted. By performing similar measurements on the gas phase of these solvents we can compare the hyperpolarizabilities in the two phases.

**Keywords:** Nonlinear optical materials, Ultrafast nonlinear optics

## 1. INTRODUCTION

The nonlinear optical (NLO) properties of solvents have been the subject of numerous studies but often result in conflicting results depending on the experimental method, pulsewidth and interpretation [1-3]. Here we use our recently developed beam deflection (BD) technique which we used to determine the response functions of carbon disulfide (CS<sub>2</sub>) [4-6] to determine the response functions of a few selected organic solvents. These response functions are useful for predicting the outcome of other NLO experiments and are particularly useful in interpreting results performed on solutions of organic dyes in solvents, i.e. to separate the response of the solute. Other methods that have been used to determine the NLO response of solvents include the optical Kerr effect (OKE) [7-10], degenerate four-wave mixing (DFWM) [11, 12], and nonlinear interferometry [2], as well as frequency domain light scattering [13], third-harmonic generation [3], and Z-scan [1, 3, 14, 15]. As is known for CS<sub>2</sub>, the NLO response of organic solvents is a combination of bound-electronic and nuclear contributions. Knowing the temporal response of each of these and their relative contributions allows the determination of the overall NLO response for a particular pulsewidth.

In this proceeding we present BD measurements to measure the temporal and polarization NLO response of a few selected organic solvents including toluene, pyridine, chloroform, carbon tetrachloride, acetonitrile and octanol, from which we derive the NLO response functions. We first give the theory of the nonlinear responses including both nearly instantaneous bound-electronic and noninstantaneous nuclear contributions, along with a brief explanation of the BD method. Polarization resolved BD measurements are performed on these solvents, from which the magnitude and temporal response of each mechanism are resolved. Finally, using the response functions the effective nonlinear refractive index ( $n_{2,eff}$ ) is predicted for different pulsewidths.

## 2. NONLINEAR REFRACTION IN ORGANIC SOLVENTS

The NLO response of an organic solvent is determined by the combined bound-electronic and nuclear contributions. While the bound-electronic response of these isotropic liquids is much faster than the femtosecond pulses used to measure it and can be described by a single nonlinear refractive index,  $n_{2,el}$ , there can be multiple nuclear contributions which can be comparable or longer than the pulsewidth used. The overall response of the change in index can then be determined by:

$$\Delta n(t) = 2n_{2,el}I(t) + \int_{-\infty}^{\infty} R(t-t')I(t')dt', \quad (1)$$

where  $I(t)$  is the irradiance and  $R(t)$  is the nuclear NLO response function. There are four primary contributors to  $R(t)$  and we follow the previous works of Refs. [2, 7, 9, 16, 17] where these contributions are treated as linearly independent:

$$R(t) = \sum_m n_{2,m}r_m(t), \quad (2)$$

where  $n_{2,m}$  is the magnitude of the  $m$ th mechanism, and the temporal response functions  $r_m(t)$  are normalized so that

$$\int_{-\infty}^{\infty} r_m(t)dt = 1. \quad (3)$$

Molecular reorientation in the presence of the electric field, which produces a torque on the molecule, is modeled as a driven damped harmonic oscillator. In the liquid state this is an overdamped oscillator described by [7]:

$$r_d(t) = C_d \left( 1 - e^{-\frac{t}{\tau_{r,d}}} \right) e^{-\frac{t}{\tau_{f,d}}} \Theta(t), \quad (4)$$

where the subscript  $d$  indicates the diffusive reorientation mechanism,  $\tau_{r,d}$  and  $\tau_{f,d}$  are the rise and fall times, respectively,  $C_d = (\tau_{r,d} + \tau_{f,d})/\tau_{f,d}^2$  is a normalization factor, and  $\Theta(t)$  is the Heaviside step-function. For molecules in the liquid state, molecular interactions become important and with this applied torque results in a rocking motion referred to as libration. The quantum harmonic oscillator model of the underdamped librational response function is given by [9]

$$r_l(t) = C_l e^{-\frac{t}{\tau_{f,l}}} \Theta(t) \int_0^{\infty} \frac{\sin(\omega t)}{\omega} g(\omega) d\omega, \quad (5)$$

where the subscript  $l$  indicates the librational mechanism and  $g(\omega)$  is the distribution function of the librational motion. As a result of the random Gaussian process, the response is inhomogeneously broadened [18], which is described by an antisymmetrized Gaussian distribution function [19]

$$g(\omega) = e^{-\frac{(\omega-\omega_0)^2}{2\sigma^2}} - e^{-\frac{(\omega+\omega_0)^2}{2\sigma^2}}, \quad (6)$$

in which  $\omega_0$  and  $\sigma$  are the center frequency and bandwidth, respectively. In addition there are collision-induced changes in the molecular polarizability described by

$$r_c(t) = C_c \left( 1 - e^{-\frac{t}{\tau_{r,c}}} \right) e^{-\frac{t}{\tau_{f,c}}} \Theta(t), \quad (7)$$

where the subscript  $c$  indicates the collision-induced nonlinearity [16]. The sum of these three nuclear responses gives the overall response for  $R(t)$ . The multiple nonlinear mechanisms would seemingly make any fitting of the nonlinear response problematic; however, the additional information from the polarization symmetry makes such fitting possible. There are two symmetries for these initially isotropic liquids. The symmetry of the bound-electronic and collision-induced mechanisms follows this isotropic symmetry of the liquid; however, the reorientation of the molecules in the polarized electric field of the laser induces an anisotropy in the liquids resulting in a very different symmetry and a different polarization dependence of the NLO response for reorientation and libration [4, 5].

### 3. BEAM DEFLECTION

We recently developed an excitation-probe technique capable of measuring the temporal dependence of the nonlinear refraction of materials in analogy with the standard excite-probe technique for measuring the light-induced changes in absorption [4-6]. This method is very similar to photothermal beam deflection but utilizes short pulse excitation along with a temporal delay line as shown in Fig. 1. The probe beam is displaced to the wing of the excitation beam where the irradiance gradient is maximum to deflect the probe beam onto a quad-cell detector. The BD signal is the difference  $\Delta E = E_{left} - E_{right}$  in energy between the left and right halves of a quad-segmented photodiode which can be normalized by the total energy  $E$  on the quad-cell. In the small signal limit,  $\Delta E(t)/E$  is nearly proportional to the refractive index change  $\Delta n(t)$  [5].

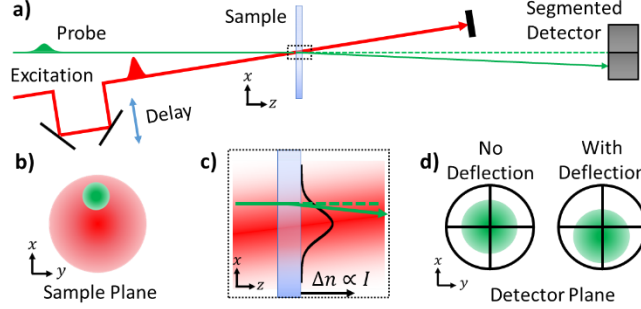


Fig. 1. a) Schematic diagram of beam deflection experiment, b) irradiance distribution of excitation (red) and probe (green) at sample plane, c) zoom in of a) at sample showing profile of  $\Delta n$ , d) probe beam on segmented detector without and with deflection. Figure taken from Ref. [4].

As derived in Ref. [4], assuming Gaussian spatial and temporal pulses, the electric field envelope at the exit surface of the sample, under the influence of the excitation induced nonlinearity, is given by:

$$\mathcal{E}(r, T) = \mathcal{E}_0(r) \exp \left( -\frac{(T + T_d - \rho)^2}{2\mathcal{T}^2} + i \frac{k_0 L}{\rho} I_{e,0}(r) \cdot \left\{ 2n_{z,el} [\text{erf}(T) - \text{erf}(T - \rho)] + \int_{T-\rho}^T \int_{-\infty}^{\infty} R(T_2 - T_1) e^{-T_1^2} dT_1 dT_2 \right\} \right), \quad (8)$$

Here the sample is assumed thin,  $I_{e,0}$  is the peak irradiance of the excitation pulse,  $T = (\mathbf{t} - \mathbf{z}/v_e)/\tau_e$  is the dimensionless normalized time that moves with the excitation group velocity  $v_e$ ,  $\tau_e$  is the excitation pulse width (HW1/eM),  $T_d$  is the dimensionless delay between excitation and probe,  $\mathcal{T} = \tau/\tau_e$  is the normalized probe pulse width, and  $L$  is the sample thickness. Since excite and probe are chosen to have different wavelengths to suppress artifacts, we account for group-velocity mismatch, GVM, and introduce the GVM parameter,  $\rho$ , so that:

$$\rho = \frac{L}{\tau_e} \left( \frac{1}{v} - \frac{1}{v_e} \right) = \frac{L}{\tau_e c} (n_g - n_{g,e}), \quad (9)$$

where  $n_g$  and  $n_{g,e}$  are the group indices of the probe and excitation, respectively. We then calculate the probe field at the quad-cell detector by Fresnel propagation from the back of the sample, and integrate over the left and right half planes to calculate  $\Delta E(T_d)/E$ .

BD data is taken for three polarization combinations to yield the tensor symmetries. Parallel polarizations give all positive contributions to the nonlinear refraction, while for perpendicular polarizations the reorientational and librational contributions

are negative. This contribution goes to zero for the so-called magic angle between the excitation and probe polarizations ( $\theta = 54.7^\circ$ ). The total induced refractive index changes are given by

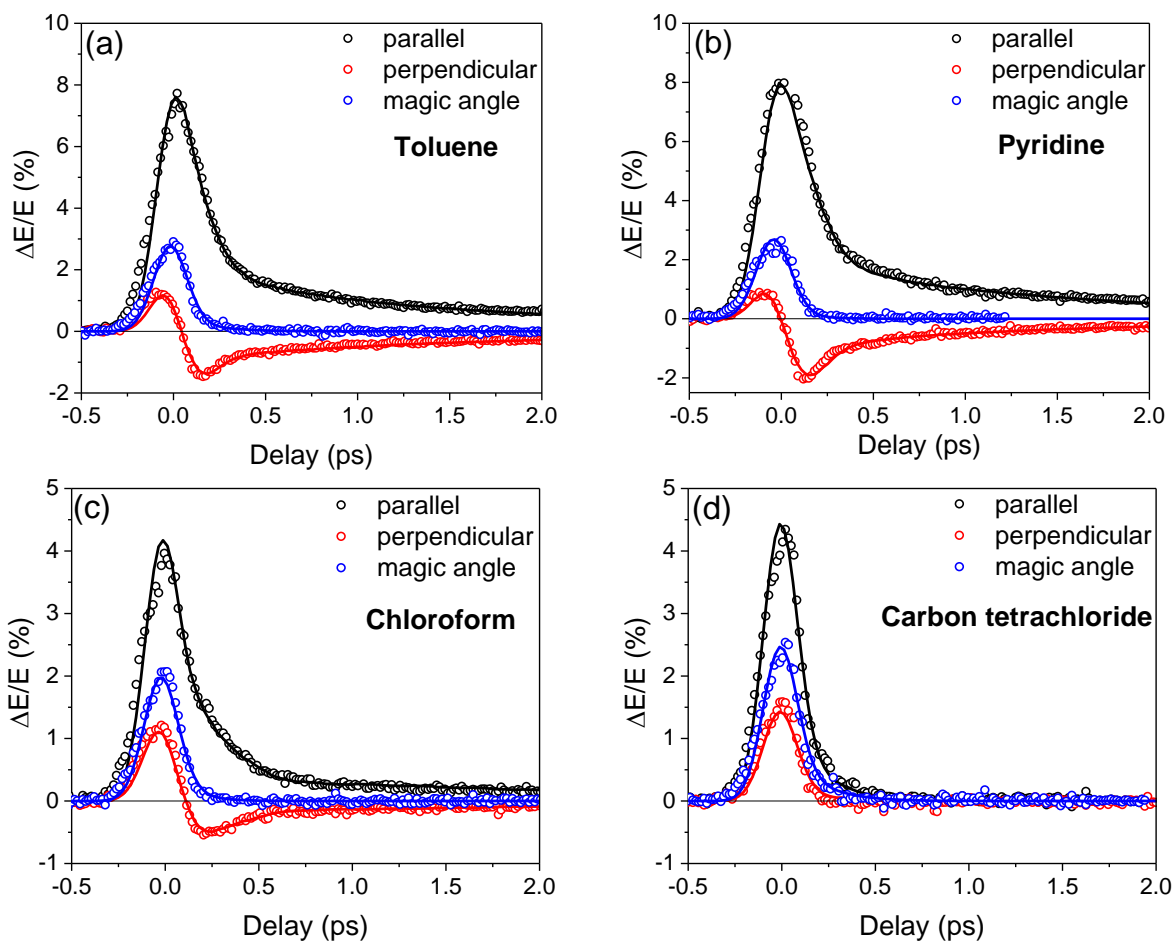
$$\Delta n(\theta) = \Delta n_{\parallel} \cos^2(\theta) + \Delta n_{\perp} \sin^2(\theta). \quad (10)$$

For isotropic symmetry,  $\Delta n_{\perp}^{iso} = \Delta n_{\parallel}^{iso}/3$ , while for reorientational,  $\Delta n_{\perp}^{re} = -\Delta n_{\parallel}^{re}/2$ . Thus the polarization dependence of the refractive index change is given by:

$$\Delta n(\theta) = \Delta n_{\parallel}^{iso} \left( \cos^2(\theta) + \frac{1}{3} \sin^2(\theta) \right) + \Delta n_{\parallel}^{re} \left( \cos^2(\theta) - \frac{1}{2} \sin^2(\theta) \right). \quad (11)$$

#### 4. EXPERIMENTAL RESULTS

In this work, BD experiments are performed using 800 nm, 150 fs (FWHM) pulses as the excitation, which are derived from a Ti:sapphire amplified system at a repetition rate of 1 kHz. A portion of the excitation is used to generate a white-light continuum (WLC) by focusing into 1 cm quartz cuvettes filled with water, which is then spectrally filtered by narrow bandpass interference filters ( $\Delta\lambda \sim 10$  nm) at 700 nm to use as the probe. The probe is detected by a quad-segmented Si photodiode (OSI QD50-0-SD) placed 25 cm behind the sample. The wavelength of the excitation and probe are chosen to be slightly nondegenerate within the transparency window of the organic solvents to avoid artifacts common in degenerate experiments [20], as well as to minimize the reduction of temporal resolution caused by GVM. The solvents were recently purchased from Sigma-Aldrich and have high purity ( $\geq 99\%$ ). The BD measurements on selected solvents are all conducted using 1 mm path length quartz cuvettes using identical experimental conditions, in which the contribution from the cuvette is measured separately and subtracted.



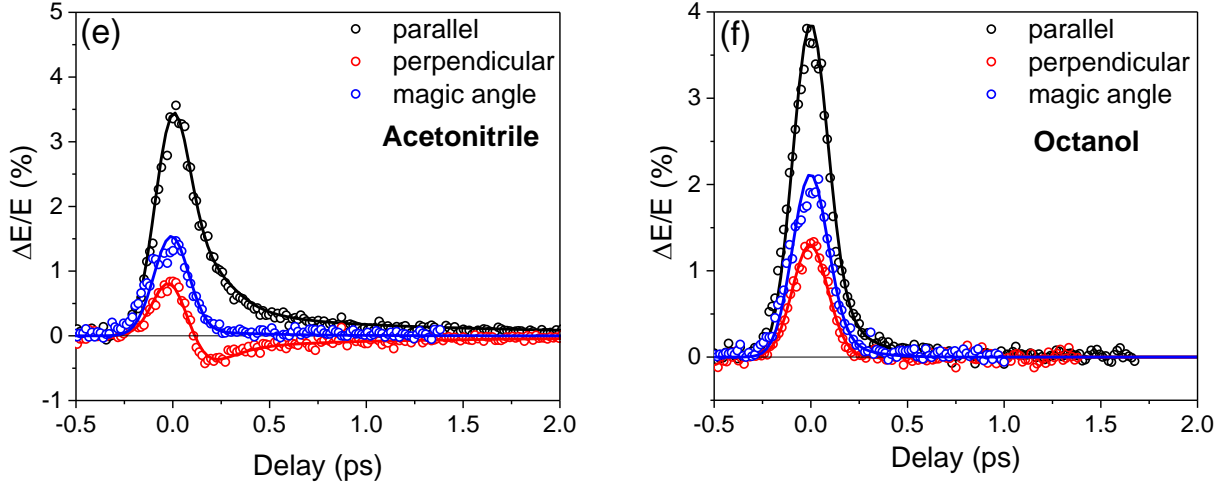


Fig. 2. Measured (circles) and fit (curves) of BD signals for a) Toluene, b) Pyridine, c) Chloroform, d) Carbon tetrachloride, e) Acetonitrile and f) Octanol with parallel (black), perpendicular (red) and magic angle (blue) polarization combinations.

Table 1. Fit parameters of response functions of solvents \*

	$n_{2,el}$	$n_{2,c}$	$\tau_{r,c}$	$n_{2,l}$	$\omega_0$	$\tau_{f,l}$	$n_{2,d}$	$\tau_{r,d}$
			$\tau_{f,c}$		$\sigma$			$\tau_{f,d}$
<b>Toluene</b>	0.58	0.12	$150 \pm 50$	0.9	$11 \pm 2$	$250 \pm 50$	2.8	$250 \pm 50$
			$150 \pm 50$		$6 \pm 2$			$1700 \pm 100$
<b>Pyridine</b>	0.6	0.02	$500 \pm 50$	1.1	$5 \pm 1$	$200 \pm 50$	2.8	$100 \pm 50$
			$100 \pm 50$		$10 \pm 2$			$1600 \pm 100$
<b>Chloroform</b>	0.41	0.08	$100 \pm 50$	0.4	$5 \pm 2$	$250 \pm 50$	0.75	$500 \pm 50$
			$100 \pm 50$		$2 \pm 1$			$1800 \pm 300$
<b>Carbon tetrachloride</b>	0.46	0.2	$100 \pm 50$	0	N/A	N/A	0	N/A
			$150 \pm 50$		N/A			N/A
<b>Acetonitrile</b>	0.31	0.05	$100 \pm 50$	0.25	$5 \pm 2$	$250 \pm 50$	0.42	$100 \pm 50$
			$150 \pm 50$		$6 \pm 2$			$1500 \pm 300$
<b>Octanol</b>	0.4	0.06	$200 \pm 50$	0.03	$2 \pm 1$	$150 \pm 50$	0	N/A
			$100 \pm 50$		$2 \pm 1$			N/A

\* $n_{2,m}$  are given in the units of  $10^{-19} \text{ m}^2/\text{W}$ ;  $\tau_{r,m}$  and  $\tau_{f,m}$  are given in units of fs;  $\omega_0$  and  $\sigma$  are given in units of  $\text{ps}^{-1}$ .

In Fig. 2, the time-resolved NLO response functions of the selected solvents are measured by BD experiment with parallel, perpendicular and magic angle polarization combinations. Similar with  $\text{CS}_2$  [4, 5], the BD signals from the anisotropic molecules including toluene, pyridine, chloroform and acetonitrile show the universal temporal dynamics, with an instantaneous response at zero delay attributable to purely electronic hyperpolarizability and the three major noninstantaneous contributions at positive delay due to intermolecular nuclear motions [4, 7, 9]. Determination of their polarization dependence from BD measurements allows unambiguous separation and determination of the NLO response function of each mechanism. Following the analysis methodology introduced in Ref. [4], based on the BD signal at the magic angle, bound-electronic  $n_{2,el}$  and a small collisional response, described by Eq. (7), can be first resolved by fitting the slightly asymmetric cross-correlation signal. Then the parallel and perpendicular results can be used together to fit the librational and reorientational responses using Eqs. (4) and (5) respectively, considering the isotropic and reorientational symmetries given in Eqs. (10) and (11). Finally, the NLO response functions are fully resolved for each of the solvent and the fit parameters defined in Eqs. (1-7) are tabulated in Table 1. Errors in  $n_{2,m}$  (~20%) are estimated from the irradiance uncertainty. The response function for highly symmetric molecules is much simpler, as the librational and reorientational effects are negligible. This can be seen by comparing the BD measurements of the less symmetrical chloroform ( $\text{CHCl}_3$ )

in Fig. 2(c) and completely symmetrical carbon tetrachloride (CCl<sub>4</sub>) in Fig. 2(d). Interestingly, octanol, as an anisotropic molecule, does not show an obvious reorientational response on the time scale of the pulsewidth, and only a small librational response is barely resolved owing to the large impact of the reorientational symmetry  $\Delta n_{\perp}^{re} = -\Delta n_{\parallel}^{re}/2$  on parallel and perpendicular results. This is probably because with large moment of inertia octanol molecules hardly rotate under the torque applied by fs pulses, resulting in a small  $n_{2,d}$ .

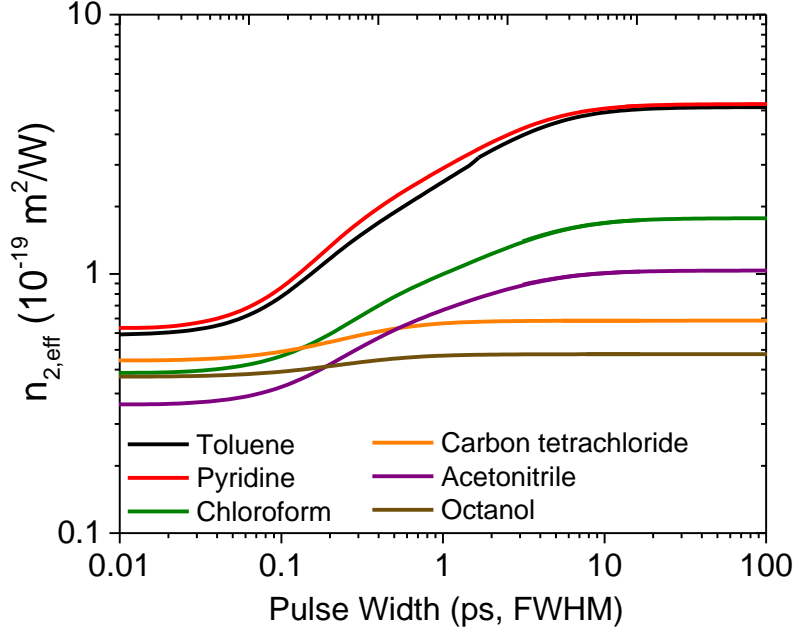


Fig 3. Calculations pulsewidth dependence of  $n_{2,eff}$  for selected solvents using NLO response function with parameters given in Table 1.

The noninstantaneous nuclear nonlinearity of organic solvents makes the effective nonlinear refractive index pulsewidth dependent. Knowing the response function of each mechanism enables the prediction of outcome of other NLO experiment such as Z-scan for different pulsewidths. As discussed in Ref. [4],  $n_{2,eff}$  is defined as

$$\Delta n(t) = n_{2,eff} I(t), \quad (12)$$

In single beam experiments such as Z-scan, the index change is averaged over the pulse irradiance, thus  $n_{2,eff}$  is related to the response function by

$$n_{2,eff} \equiv n_{2,el} + \frac{\int_{-\infty}^{\infty} I(t) \int_{-\infty}^{\infty} R(t-t_1) I(t_1) dt_1 dt}{\int_{-\infty}^{\infty} I^2(t) dt}, \quad (13)$$

Using the response function determined by BD measurements, Eq. (13) gives excellent prediction of the outcomes of pulsewidth dependent Z-scan measurements for CS<sub>2</sub> [4]. Based the same methodology,  $n_{2,eff}$  of the selected solvents are calculated for different pulsewidths in Fig 3 using the values given in Table 1. For short pulses (< 50 fs), only bound electronic nonlinearity contributes significantly ( $n_{2,eff} = n_{2,el}$ ) due to its nearly instantaneous nature. The noninstantaneous nuclear nonlinearities, particularly librational and reorientational responses, can increase or even dominate  $n_{2,eff}$  for longer pulsewidths. For example,  $n_{2,eff}$  of toluene and pyridine at longer pulsewidths (>10 ps) increases nearly 8× over the short pulse limit, primarily owing to their large  $n_{2,l}$  and  $n_{2,d}$ . Carbon tetrachloride and octanol with small or negligible  $n_{2,l}$  and

$n_{2,d}$  do not show considerable increase of  $n_{2,eff}$ . Other NLO experiments such as Z-scan can be used to verify such predictions from BD measurements.

## 5. GASES

Work is continuing on measuring these same solvents in the gaseous state using a thick heated cell. We have already measured carbon disulfide ( $\text{CS}_2$ ) [6]. In those measurements we were able to differentiate the ultrafast bound-electronic response by measuring the polarization dependence as shown in Fig. 4. For gases the nuclear responses are insignificant for the magic angle polarization. Thus we are able to extract the second hyperpolarizability,  $\gamma$ . We are then able to compare this  $\gamma$  with that obtained from the liquid measurements. However, in liquid form we need to correct for the local field which for the third-order nonlinear response for the liquid of index 1.62 is a factor of  $f^{(3)} = 5.35$ . Thus we find (as reported in Ref. [4, 6], that  $\gamma_{\text{liquid}} = 23 \pm 5 \times 10^{-62} \text{ C}^4 \text{m}^4 / \text{J}^3$ , while for the gas we find  $\gamma_{\text{gas}} = 19 \pm 3 \times 10^{-62} \text{ C}^4 \text{m}^4 / \text{J}^3$ . These values agree within errors. It will be interesting to see if the same is true for polar molecules.

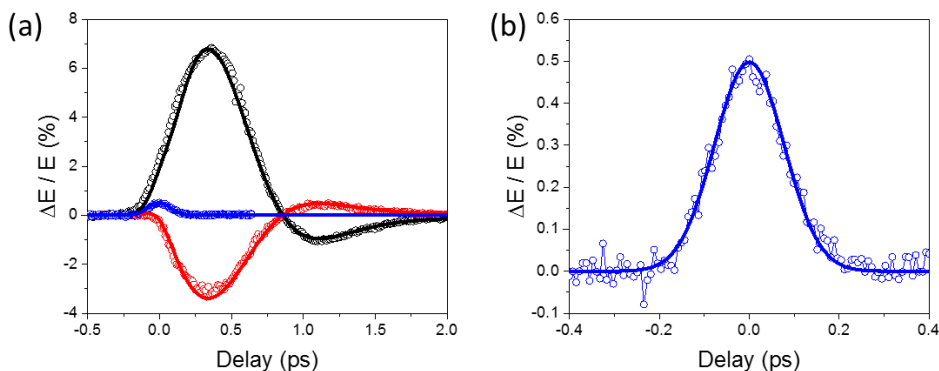


Fig. 4. (a) BD (circles) measurements of  $\text{CS}_2$  about zero delay with (curves) fits for (black) parallel, (red) perpendicular, and (blue) magic angle polarizations. (b) Zoomed in measurement at the magic angle. Taken from Ref. [6].

## 6. CONCLUSION

We have experimentally determined the total NLO response function for selected organic solvents using polarization resolved beam deflection technique, in which bound-electronic and each nuclear contributions are explicitly separated. For molecules having a permanent polarizability anisotropy such as  $\text{CS}_2$ , toluene, pyridine, acetonitrile and chloroform, NLO response function can be universally decomposed into a nearly instantaneous bound-electronic response, along with three noninstantaneous nuclear contributions which is mainly attribute to collision, libration and diffusive reorientation. The librational and reorientational responses vanish for highly symmetric molecules such as carbon tetrachloride. An exception is octanol which only shows negligible reorientational response although it is an anisotropic molecule. Knowing the parameters of each response, the  $n_{2,eff}$  is calculated for pulsewidth dependence, which can be used as predictions for the outcome of other NLO experiment such as Z-scan. We purpose to embark on characterizations of the NLO response for most commonly used organic solvents to establish self-consistent references for various NLO applications.

## 7. ACKNOWLEDGEMENT

This work was supported by the National Science Foundation grants ECCS-1202471 and ECCS- 1229563. Research was sponsored by the Army Research Laboratory and was accomplished under Cooperative Agreement Number W911NF-15-2-0090. The views and conclusions contained in this document are those of the authors and should not be interpreted as representing the official policies, either expressed or implied, of the Army Research Laboratory or the U.S. Government. The U.S. Government is authorized to reproduce and distribute reprints for Government purposes notwithstanding any copyright notation herein.

## REFERENCES

1. Iliopoulos, K., et al., *Ultrafast third order nonlinearities of organic solvents*. Optics Express, 2015. **23**(19): p. 24171-24176.
2. Yasuhiro Sato, Ryuji Morita, and Mikio Yamashita, Study on Ultrafast Dynamic Behaviors of Different Nonlinear Refractive Index Components in CS<sub>2</sub> Using a Femtosecond Interferometer. Japanese Journal of Applied Physics, 1997. **36**(4R): p. 2109.
3. Rau, I., et al., Comparison of Z-scan and THG derived nonlinear index of refraction in selected organic solvents. Journal of the Optical Society of America B, 2008. **25**(10): p. 1738-1747.
4. Reichert, M., et al., Temporal, spectral, and polarization dependence of the nonlinear optical response of carbon disulfide. Optica, 2014. **1**(6): p. 436-445.
5. Ferdinandus, M.R., et al., Beam deflection measurement of time and polarization resolved ultrafast nonlinear refraction. Optics Letters, 2013. **38**(18): p. 3518-3521.
6. Reichert, M., et al., Beam deflection measurement of bound-electronic and rotational nonlinear refraction in molecular gases. Optics Express, 2015. **23**(17): p. 22224-22237.
7. McMorrow, D., W.T. Lotshaw, and G.A. Kenney-Wallace, *Femtosecond optical Kerr studies on the origin of the nonlinear responses in simple liquids*. Quantum Electronics, IEEE Journal of, 1988. **24**(2): p. 443-454.
8. Ho, P.P. and R.R. Alfano, *Optical Kerr effect in liquids*. Physical Review A, 1979. **20**(5): p. 2170-2187.
9. McMorrow, D., et al., Analysis of Intermolecular Coordinate Contributions to Third-Order Ultrafast Spectroscopy of Liquids in the Harmonic Oscillator Limit. The Journal of Physical Chemistry A, 2001. **105**(34): p. 7960-7972.
10. Zhong, Q. and J.T. Fourkas, *Optical Kerr Effect Spectroscopy of Simple Liquids†*. The Journal of Physical Chemistry B, 2008. **112**(49): p. 15529-15539.
11. Xu, Q.-H., Y.-Z. Ma, and G.R. Fleming, Heterodyne detected transient grating spectroscopy in resonant and non-resonant systems using a simplified diffractive optics method. Chemical Physics Letters, 2001. **338**(4-6): p. 254-262.
12. Steffen, T., J.T. Fourkas, and K. Duppen, *Time resolved four- and six-wave mixing in liquids. I. Theory*. The Journal of Chemical Physics, 1996. **105**(17): p. 7364-7382.
13. Bloembergen, N. and P. Lallemand, Complex Intensity-Dependent Index of Refraction, Frequency Broadening of Stimulated Raman Lines, and Stimulated Rayleigh Scattering. Physical Review Letters, 1966. **16**(3): p. 81-84.
14. Sheik-Bahae, M., et al., *Sensitive measurement of optical nonlinearities using a single beam*. Quantum Electronics, IEEE Journal of, 1990. **26**(4): p. 760-769.
15. Yan, X.-Q., et al., Third-order nonlinear susceptibility tensor elements of CS<sub>2</sub> at femtosecond time scale. Optics Express, 2011. **19**(6): p. 5559-5564.
16. Bucaro, J.A. and T.A. Litovitz, *Rayleigh Scattering: Collisional Motions in Liquids*. The Journal of Chemical Physics, 1971. **54**(9): p. 3846-3853.
17. Greene, B.I., et al., Microscopic dynamics in simple liquids by subpicosecond birefringences. Physical Review A, 1984. **29**(1): p. 271-274.
18. Kalpouzos, C., et al., *Femtosecond laser-induced optical kerr dynamics in CS<sub>2</sub>/alkane binary solutions*. Chemical Physics Letters, 1988. **150**(1): p. 138-146.
19. Friedman, J.S. and C.Y. She, The effects of molecular geometry on the depolarized stimulated gain spectra of simple liquids. The Journal of Chemical Physics, 1993. **99**(7): p. 4960-4969.
20. Dogariu, A., et al., *Purely refractive transient energy transfer by stimulated Rayleigh-wing scattering*. Journal of the Optical Society of America B, 1997. **14**(4): p. 796-803.